Analytical model for blood glucose detection using electrical impedance spectroscopy

Bruna Gabriela Pedro, John Alexander Gomez Sanchez, Pedro Bertemes-Filho

PII: S2214-1804(24)00080-1

DOI: https://doi.org/10.1016/j.sbsr.2024.100698

Reference: SBSR 100698

To appear in: *Sensing and Bio-Sensing Research*

Received date: 27 June 2024

Revised date: 19 September 2024

Accepted date: 24 September 2024

Please cite this article as: B.G. Pedro, J.A.G. Sanchez and P. Bertemes-Filho, Analytical model for blood glucose detection using electrical impedance spectroscopy, *Sensing and Bio-Sensing Research* (2024), https://doi.org/10.1016/j.sbsr.2024.100698

Analytical Model for Blood Glucose Detection Using Electrical Impedance Spectroscopy

Bruna Gabriela Pedro[a], John Alexander Gomez Sanchez[b], Pedro Bertemes-Filho[a,1]

[a]State University of Santa Catarina, Dept. Electrical Engineering, Joinville, Brazil

[b]CaliYuk Enterprises, Bogota, Colombia

Abstract

The article presents a preclinical study focused on developing a non-invasive blood glucose monitoring device. Current glucose monitoring methods, such as capillary or venous tests, are inconvenient for frequent use, making continuous monitoring challenging. This study explores the BGP (Bruna Gabriela Pedro) model, which links electrical impedance to blood glucose levels, as a potential alternative. Using the Geselowitz Theorem and impedance spectroscopy in a 4-electrode configuration, the study investigates the relationship between blood conductivity and glucose concentration. Impedance spectra were recorded for five human blood samples with glucose concentrations between 106 and 188 mg/dL. These samples were housed in an insulating container with four stainless steel electrodes. Conductivity was calculated using the Geselowitz Theorem at 1.0, 3.9, and 24.9 kHz. A finite element model built in COMSOL was employed to assess electrode sensitivity, which had a maximum regression error of 3.75%. The results demonstrated a sigmoid relationship between blood glucose concentration and conductivity, with impedance decreasing non-linearly as glucose levels increased. Sensitivity diminished for glucose concentrations exceeding 188 mg/dL. An increase of 82 mg/dL in glucose concentration led to conductivity

*Corresponding author

[1]Email: pedro.bertemes@udesc.br

changes of 1.14, 2.82, and 5.14 S/m at frequencies of 1.0, 3.9, and 24.9 kHz, respectively. The findings suggest that the BGP analytical model could be refined through the inclusion of additional data on glucose's impact on electrical impedance. These improvements could support the development of non-invasive glucose meters. The research holds significant clinical potential for the creation of a simple, cost-effective glucose monitoring device. Continuous glucose monitoring could enhance diagnostic accuracy and support better therapeutic decision-making, particularly in emergency care. The affordability and accessibility of such a device may benefit a broad patient base.

Keywords: BGP model, COMSOL, Electrical impedance spectroscopy, Geselowitz theorem, Sensibility

1. Introduction

The accurate characterization of human blood with respect to various parameters is essential for medical applications, including the estimation of hematocrit, erythrocyte sedimentation rate, and cardiac output [1]. Diabetes, now one of the top ten causes of death globally, has seen a significant rise in mortality over the past decade [2]. While preventive measures are critical, they are complicated by autoimmune dysfunctions [3]. Continuous monitoring is necessary but often impractical with invasive techniques, such as hair testing and colorimetric enzyme testing [4]. Frequent finger pricks, commonly required for those with severe diabetes relying on hair tests, present a costly, painful, and inconvenient method [5].

Current blood glucose monitoring methods include invasive techniques like venipuncture and capillary testing. Semi-invasive techniques, such as fixed sensors, penetrate the interstitial

skin layer [6]. Although venipuncture with colorimetric tests is the gold standard for reliability, it is not feasible for routine monitoring [7]. Capillary tests, while repeatable, cause discomfort and are prone to measurement errors, including issues with sample size and high test strip costs [8]. Semi-invasive devices, which measure interstitial fluid, are expensive and may not always complete the intended monitoring cycle, raising concerns about safety and reliability [8, 9].

The glycated hemoglobin test, which measures glucose molecules bound to hemoglobin [6], also falls short for daily monitoring. Recent advancements in non-invasive and continuous glucose monitoring, including wearable technologies like smartwatches, offer potential solutions. Chang et al. [10] have explored such devices based on semi-infinite diffusion models, though these have not yet reached commercial production. Given the high healthcare costs (US$760 billion in 2019, projected to reach US$825 billion by 2030) [2], there is a pressing need for cost-effective non-invasive glucose monitoring solutions.

Optical [4], microwave [11], electrochemical [4] and electrical impedance spectroscopy [12] techniques have been investigated for non-invasive blood glucose detection. The primary challenge is to correlate measurable parameters with biological behavior at the cellular level to develop a physically significant model. The conductivity of human blood at low frequencies is critical for designing numerical simulations for radio-frequency and pulsed electric field ablation treatments [13]. While artificial neural networks (ANNs) have also been widely used in non-invasive blood glucose measurement devices [12], imposing an advantage into comparison to analytical models (AM). Although AMs are more complex, they have some benefits such as detailed behavioral prediction and error propagation management.

Our previous published work proposed an analytical model for blood conductivity related to glucose changes [14]. The objective of this work is to enhance the BGP analytical model of

blood glucose concentration and its correlation with impedance spectroscopy measurements by using *in-vitro* human samples.

2. Methodology

BGP analytical model

The BGP model expresses the electrical impedance modulus ($|Z|$) as a function of glucose concentration [14]. The primary application of this model is in the development of non-invasive glucose monitoring devices, specifically through electrical bioimpedance spectroscopy. While the model describes impedance behavior in an *in-vivo* experiment, understanding the individual behavior of parameters affected by glucose variations would enable a more comprehensive characterization. This would allow the BGP model not only to describe the behavior but also to predict it.

The model is based on the assumption that human blood is a two-phase composite made up of a conductive main matrix and non-conductive particles that simulate blood glucose. Our previous work showed that glucose, inside an ionic medium, exhibits a dual behavior, either increasing and decreasing the conductivity of the medium. These results showed that blood conductivity cannot be simulated merely by Bruggeman's model and then it should be furthered investigated [15]. The original version of the BGP model is expressed as:

$$|Z| = \sqrt{\left(\frac{L^2}{A^2}\frac{1}{\sigma_h^2}\frac{1}{(1-k-k')^3}\right) + \frac{(L - j2\pi\tau Lf)^2}{f^2\left\lfloor 2\pi A(\varepsilon_\infty + \Delta\varepsilon) - 4\pi^2 A\varepsilon_\infty j\pi\tau f) + \right\rfloor^2}} \quad (1)$$

where σ_h is the conductivity of the blood plasma and k' is the volume fraction of glucose in the volume.

Modeling according to Geselowitz's theorem

Geselowitz's theorem states that an impedance change ΔZ is directly proportional to a negative change in conductivity $\Delta\sigma$:

Figure 1: Measuring set up modelled in COMSOL using 4 punctual electrodes, where VCCS is a voltage controlled current source, V_{CD} is the measuring voltage across electrodes C and D.

$$\Delta\sigma = -\Delta Z.S \tag{2}$$

where S is the sensitivity which converts impedance into conductivity. Sensitivity is directly related to the geometry of the electrodes and the distance between the element of the volume conductor, where the change in conductivity occurs, and the electrodes on the surface of this volume [16].

Figure 1 shows a homogeneous and semi-infinite medium subjected to an impedance measurement. According to the Geselowitz's theorem [16], the differential change in transfer impedance T_z is given by the ratio the measured potential and the applied current ($T_z = \frac{V_{CD}}{I}$). The measuring voltage between electrodes $C:D$ (V_{CD}) is produced by the injecting current I between electrodes $A:B$, which means of a voltage controlled current source V_{CCS}. The measuring voltage V_{CD} can be given by:

$$V_{CD} = \frac{1}{2\pi\sigma}\left(\frac{1}{R_{AC}} - \frac{1}{R_{AD}} + \frac{1}{R_{BC}} - \frac{1}{R_{BD}}\right) \tag{3}$$

Considering a uniform, homogeneous and semi-infinite medium, and point source electrodes, then

the electrical conductivity of the medium can be described as:

$$\sigma = \frac{1}{2\pi T_z}\left(\frac{1}{R_{AC}} - \frac{1}{R_{AD}} + \frac{1}{R_{BC}} - \frac{1}{R_{BD}}\right) \tag{4}$$

where R_{AC} is the distance between electrodes A and C, R_{AD} is the distance between electrodes A and D, R_{BC} is the distance between electrodes B and C, and R_{BD} is the distance between electrodes B and D.

Based on the Geselowitz's theorem and rewriting equation 2, the sensitivity for an infinitesimal unit of volume (voxel) is given by:

$$S_i(\mathbf{r}, \rho) = \mathbf{J}(\mathbf{r}, \mathbf{r}_{A,i}, \mathbf{r}_{B,i}) \cdot \mathbf{J'}(\mathbf{r}, \mathbf{r}_{C,i}, \mathbf{r}_{D,i}) \tag{5}$$

where $\mathbf{J}$ and $\mathbf{J'}$ are the current densities generated by electrodes $A:B$ and $C:D$, respectively, $\mathbf{r}_{A,i}$ and $\mathbf{r}_{B,i}$ are the distances between the voxel i and the injecting electrodes, whereas $\mathbf{r}_{C,i}$ and $\mathbf{r}_{D,i}$ are the distances related to the measruing electrodes.

In order to better explore this equation, we have used the COMSOL [17] aiming to analyze the sensitivity of a tetrapolar impedance probe and to investigate limiting factors which might impact when dealing with in-vitro experiment. COMSOL is a general-purpose simulation software based on advanced numerical methods containing a coupled multiphysics and single-physics modeling capabilities. The sensitivity equation can be described as:

$$S = (ec.Jx \cdot ec2.Jx + ec.Jy \cdot ec2.Jy + ec.Jz \cdot ec2.Jz) \tag{6}$$

where $ec.Jx$, $ec.Jy$, and $ec.Jz$ are the components of the current density vector of the current injection electrodes (e.g., electrodes $A:B$ in Figure 1), and $ec2.Jx$, $ec2.Jy$, and $ec2.Jz$ are the components of the induced current density vector of the voltage measurement electrodes (e.g., electrodes $C:D$ in Figure 1). All the model parameters and boundary conditions for COMSOL

simulations can be seen in the complimentary files of this manuscript.

Figure 2: Sample box for measurements. It was printed with an insulating material with dimensions of $12.45\,\text{mm} \times 12.45\,\text{mm} \times 6.35\,\text{mm}$ (LxAxH).

Experimental Measurements

In this article, the sample preservation during 2 hours follows the standard procedures for clinical laboratory. Fluoride tubes were used to collect human blood for the *in-vitro* experiment. Fluoride acts as a glycolytic inhibitor and has a sufficient anticoagulant effect during the interval between sample collection and measurement. The colorimetric enzymatic test was used to make five blood samples, each one corresponding to a point of the glycemic curve. The initial sample was taken from a volunteer who was fasting, and the other four were obtained after ingesting 75 grams of anhydrous dextrose (glucose) at 30, 60, 90, and 120 minutes.

Figure 2 shows a disposable plastic box that was printed with a non-conductive material sizing 12.45x12.45x6.35 mm. The electrodes material are made of stainless steel (type AISI 304 - American Iron and Steel Institute) of 0.18 mm diameter and equally spaced 5.08 mm apart between center.

The MFIA (Multi Frequency Impedance Analyser from Zurich Instruments) measures both modulus an impedance phase of the samples in a range of 10 Hz to 1 MHz. The process was repeated 5 times for stability purpose. The container shown in Figure 2 was filled with (1 mL) of blood. Distilled water was used to clean up the container prior to each measurement, and a paper towel was used to remove all moisture during sanitizing.

3. Results

Figure 3 shows that the glucose impose a dispersion in the electric field created by the injecting current in the medium, which might be related to a capacitive behavior. It can be observed that the impedance decreases as increasing glucose concentration, which was also pointed by [14]. The linear slope might be explained by a double-layer capacitance and a transfer resistance [18] in the range of 100 *Hz* to 10 *kHz*.

Figure 3: Impedance modulus as a function of frequency for different blood glucose concentrations.

The chosen frequencies for running 2 were selected randomly in order to calculate $|Z|$. Figure 4 shows a sigmoid behavior of the conductivity into respect to the glucose volumetric ratio of the blood. It must be emphasized that the frequencies were chosen based on the modelling adopted in this article. Therefore, based both on the impedance measurements and modelling technique, it was selected by convenience a linear range between 1 and 24.5 kHz. The equations $f(k')$, $g(k')$ and $h(k')$ are the curve regressions for 1, 3.9 and 24.9 *kHz*, respectively. The conductivity $\sigma(k')$ as a function of the glucose volume fraction k' can be calculated by:

Figure 4: Curves for conductivity as a function of the volume fraction of blood glucose.The equations $f(k')$, $g(k')$ and $h(k')$ are the curve regressions for 1, 3.9 and 24.9 *kHz*, respectively.

$$\sigma(k') = \frac{a}{(1+be^{c-dk'}))} + g \tag{7}$$

where a, b, c, d and g are coefficients.

The simulated conductivity was calculated using the coefficients found in $h(k')$, according to equation 8, with a maximum error of 3.75%.

$$\sigma(k') = \frac{0.0545}{(1+14.94e^{21.80-19,500k'}))} + 0.0015 \tag{8}$$

The sensitivity distribution within the volume conductor (e.g. the container shown in figure 2) was calculated using Geselowitz's theorem for different glucose concentrations by using the equation 6 [19]. Figure 6 shows both positive and negative areas, where the positive one is called focused zone as defined in [20]. The figure shows symmetry in both yz and xz planes. It can be observed that the number of pixels of positive sensitivity increases as increasing the glucose concentration up to a saturation value of 188 *mg*/*dl*. The pixels with maximum negative sensitivity also increases, but in a lesser extent, along the peripheral area of the volume conductor.

Figure 5: XY plane sensitivity upon glucose concentrations. (a) 106 *mg*/*dL*. (b) 123 *mg*/*dL*. (c) 132 *mg*/*dL*. (d) 188 *mg*/*dL*.

Figure 6: XZ plane sensitivity upon glucose concentrations. (a) 106 *mg*/*dl*. (b) 123 *mg*/*dl*. (c) 132 *mg*/*dl*. (d) 188 *mg*/*dl*.

The simulation results also permits to analyze the variation of both conductivity parameters and glucose concentration in a time domain. Figure 7 shows the relationship of both conductivity and glucose concentration changes into respect to time.

Figure 7: Variation of conductivity and glucose concentration in relation to time.

4. Discussion

Correlation between impedance and glucose

Figure 3 shows that $|Z|$ is inversely proportional to the glucose concentration. This finding agrees with the data used in the work published by [14]. However, for a fixed frequency, the behavior of $|Z|$ versus k' was found to be non-linear in this work. The non-linearity might be explained by a faradaic redox reaction of H_2O_2 on the surface of the AISI 304 electrode [21], which might exhibits a catalytic activity based on the constitutive transition metal. It is also important to mention that the AISI 304 contains manganese which reacts with hydrogen peroxide improving the electrochemical reaction, as fully described at https://doi.org/10.1016/j.snb.2021.130552.

It was observed that the tetrapolar configuration of the electrodes at low glucose concentrations ($<132 mg/dl$) showed small increase in the sensitivity (Figures 6 and 5). At higher glucose concentrations, the fluid reaches the limit of ionic mobility becoming saturated and then, stops the sensitivity to increase. The geometric factor of the electrode limits the sensitivity distribution inside the volume conductor [22], as observed in figures 6 and 5. This limitation might be related to the oscillation or reorientation of the ionic charges due to the electrostatic forces in the volume, and to the reorganization of the atomic structures of the sample on the electrode surface [23].

Glucose becomes non-conductive and poorly ionizable when it is added into water,

contributing to an increase in resistivity [24]. This might be the case when the increasing in blood glucose decreases the conductivity of the total fluid. However, glucose becomes polarizable through the process of glycolysis [25], generating an organization of the molecules that reduces the probability of charge carrier collisions and, then, contributing to ionic mobility [26].

This process of breaking down the glucose molecule not only makes it polar, but also increases the number of ions in the solution. During the process, the glucose is transported into the red blood cell which activates the sodium-potassium pump which, in turns, increases the number of ions until the solution becomes saturated. Saturation occurs at the peak of glucose concentration, where insulin reaches its highest levels, thereby promoting glycolysis and regulating electrolyte balance in the blood [27]. As the ion concentration in the solution increases significantly, the portion allocated for polarization decreases, in accordance with the principle of energy conservation in the system. This could explain why the inflections of the $|Z|$ curve in Figure 3 shift along glucose concentration increases [28]. According to the results presented here, this inflection occurs at 10 *kHz* for 188 *mg*/*dl*, at 100 *kHz* for 123 *mg*/*dl*, while any change in the spectra was observed for 106 *mg*/*dl*.

It can also be observed in figure 3 that the variation of $|Z|$ tends to zero when glucose concentrations increase. This limitation is due to the electrode geometry array, as shown in figure 6. Therefore, the bench test performed in this work is not suitable for blood samples with glucose concentrations greater than 188 *mg/dl*. For tangible value in diabetic blood (> 300 *mg/dl*), the electrode geometry array shoudl be changed accordingly. Based on the measuring technique and on the electrode geometry, our coplanar tetrapolar design limited values higher than 188 mg/dl. One solution would be the use of concentric electrode geometry due to the linearity of the electric field near by the electrode's effective zone [23].

Correlation between conductivity and glucose

Analysis of figure 4 and the physical interpretation of equation 7 reveal points of agreement and disagreement with the original BGP model, which can described by:

$$\sigma(k') = k'.\frac{1}{\sqrt{1+k'^2}} \tag{9}$$

The first part of equation 9 shows that glycolysis and the potassium pump phenomenon increase ion levels in the plasma. This would justify the increase in conductivity as glucose concentration in the blood rises, which disagrees with the original BGP model. In the second part, glucose in the blood should be considered as a large molecule that becomes ionizable after glycolysis. Due to its larger size compared to ions, glucose does not contribute significantly to charge transport and stores less energy for polarization as glucose levels peak (note that polarization impedance decreases with increasing glucose levels).

Figure 8 shows the resulting curve by subtracting k' from $\sqrt{1+k'^2}$, which shows the increasing response of the conductivity as increasing the glucose inside the solution.

Figure 8: Curve resulting from the subtraction of the plots that make up the conductivity exemplified in the equation 9.

Impact of results

In an analytical model, the relationship between variables is typically expressed using equations that quantify how one parameter affects another. These equations may involve simple linear relationships or more complex non-linear interactions, depending on the nature of the

system being modeled. Regarding the relationship between blood glucose and electrical impedance spectroscopy (EIS) data, k' as a function of conductivity ($k'(\sigma)$) can be calculated by first converting $|Z(\sigma)|$ to $|Z(k')|$, and then obtaining $|Z(\sigma)|_i$ by using EIS data, where i is the impedance index for each discrete frequency f_i. Once f_i values are pre-established, σ_i can be calculated for each respective frequency. All conductivity values ($\sigma_1 \approx \sigma_2 \approx .... \approx \sigma_n$) are then summed for averaging calculation. finally, the mean conductivity is inserted into equation 7 in order to obtain k' as a function of conductivity ($k'(\sigma)$).

For prediction purpose, figure 7 might be used to investigate the analyzed quantities upon time. For instance, by knowing $\sigma(t)$ and $\sigma(t+\Delta t)$, assuming that $\Delta t \to \delta t$, the rate $\frac{\delta\sigma}{\delta t}$ can be calculated. This last, leads to predict how glucose concentration varies into respect to time ($\frac{\delta k'}{\delta t}$). By using equation 7 considering the time variation of conductivity ($\frac{\delta\sigma}{\delta t}$), then time changes of k' ($\frac{\delta k'}{\delta t}$) can be predicted. This might be the case for any intervention by the user/patient of such measuring device due to a glycemic abnormality, avoiding hypo/hyperglycemia.

In a more realistic case, equation 7 can be used in the BGP model, such that:

$$|Z|_{blood} = \frac{L}{A}\sqrt{\left(\frac{1+b.e^{c-dk'}}{a+g(1+be^{c-dk'})}\right)^2 + \left(\frac{1}{4\pi^2\varepsilon^2}\frac{1}{f^2}\right)} \qquad (10)$$

where L and A are the length and cross-sectional area of the vessel, respectively.

Figure 9 shows a proposed setup for in vivo measurements. The external current ($i_{external}$) is injected by electrodes 1 and 6 for blood investigations and an internal current ($i_{resting}$) by electrodes 2 and 5 for bones, sin, nerves and fat tissue investigations. This might allow measuring the surface layer that corresponds to $|Z|_{resting}$ ($=V/i_{resting}$), whereas $|Z|_{external}$ ($=V/i_{external}$) to deeper

materials/tissues within the sample. Both $|Z|_{external}$ and $|Z|_{resting}$ is then used to calculate k' proposed in this model.

By the fact that $|Z|_{blood} = |Z|_{external} - |Z|_{resting}$, then equation 10 can be used to describe k' as:

$$k' = \frac{c - ln\left[\frac{(a+g)M-1}{b(1-gM))}\right]}{d} \tag{11}$$

where the frequency f is pre-established for each acquisition data, L and A depend on the geometry of the electrodes, the coefficients a, b, c, d and g must be clinically calibrated for each patient.

$$M = \left[\left(\frac{A}{L}|Z|_{blood}\right)^2 - \left(\frac{1}{4\pi^2\varepsilon^2}.\frac{1}{f^2}\right)\right]^{\frac{1}{2}} \tag{12}$$

Figure 9: Schematic diagram of a proposed measuring system to better predict the glucose concentration in deep tissue by using six electrodes.

Sensitivity analysis in COMSOL

Figures 3 and 4 showed a glucose concentration saturation above 145 *mg*/*dl*, which might be due to either electrode geometry or sensitivity. It means that the displacement of electrodes in the measuring device plays a great importance in the accuracy of the model when predicting glucose concentration from EIS data.

Figure 6 indicates impedance changes in the volume surrounding the electrodes. In addition, the correct interpretation of both positive and negative sensitivity allows us to analyze whether the BGP model is being correctly used in terms of blood glucose upon conductivity.

According to [20], both negative and positive sensitivity, close to their maximums, may lead to a misinterpretation saying that conductivity is inversely proportional to impedance, or vice versa. These behaviors can be observed in figure 3, where impedance decreases as increasing glucose concentration, and in figure 4 which shows that conductivity increases as increasing the glucose concentration. This confirms the reliability of the results presented here, which agrees with the BGP model.

The results showed that the sensitivity can be used as a parameter to measure electrode saturation, as shown in figure 6. The size variation of the sample may lead to a reduction in the sensitivity for a chosen geometry. Therefore, simulations can be used to find the best geometry for a specific application. It must be highlighted the manner how sensitivity is calculated in this work. As described in [29] and [30], the sensitivity is calculated by using a pair of current electrodes to induce the electrical field in the volume conductor and calculating the resulting field using the same pair of electrodes. The use of only current electrodes in the simulation does not represent in vivo/vitro experiments, therefore voltage electrodes for picking up the measuring electrical field should be used in the simulations.

The complete instructions proceedings used to build the model in COMSOL are present in the supplement file of this article. This shows how we have simulated voltage electrodes from the potential difference generated by the current injection electrodes.

5. Conclusion

We intended to improve the model by describing the conductivity with more accuracy as a function of glucose concentration. Originally, conductivity is described by the Bruggeman model assuming simple composites, such as lactated Ringer's solution and albumin [1]. However, it does

not take into account the complexities of human blood due to glycolysis and protein glycation. Therefore, when using human blood is necessary to consider changes by the electrolytes triggered by the introduction of glucose. This work presented a description of conductivity as a function of glucose concentration in order to improve the original BGP model for non-invasive glucose measuring systems. These findings might be led to a better physical interpretation of the microscopic phenomena involved in vivo/vitro measurements, and to better explain why impedance and conductivity are altered by changing the sample user study.

The addition of glucose to *in vitro* samples may not characterize the real phenomena, as chemical reactions and metabolic changes were not considered in this work. Care should be taken when comparing the finds here to the ones get in real blood glucose measurements. However, the data obtained to establish the relationship between the blood conductivity of health volunteer and the concentration of blood glucose has proven to be reliable into respect to sensitivity simulations.

Electrode sensitivity should be used to map whether the electrode configuration is capable of measuring the range of variation for a given parameter. It was shown that a coplanar electrode geometry using a tetrapolar configuration proved to be efficient for a maximum glucose concentration of 188 *mg*/*dl*. Future work will involve analyzing the sensitivity of concentric configurations, as the electrical field is more uniform and linear within the voxels close to the electrodes. Further experimental texts with healthy and diabetic blood samples will also be necessary to calculate repeatability and accuracy.

It can be concluded that the original BGP model was optimized and can be calculated by equation 10. We believe that the optimized model might be useful for the development of non-invasive glucose measuring systems.

Acknowledgment

This study was financed in part by the Coordenação de Aperfeiçoamento de Pessoal de Nível Superior – Brasil (CAPES) – Finance Code 001. We also thank the Santa Catarina State University (UDESC) and FAPESC for both institutional and financial support.

References

[1] T. Alexy, J. Detterich, P. Connes, K. Toth, E. Nader, P. Kenyeres, J. Arriola-Montenegro, P. Ulker, M. J. Simmonds, Physical properties of blood and their relationship to clinical conditions, Frontiers in Physiology 13 (2022) 906768.

[2] R. Williams, S. Karuranga, B. Malanda, P. Saeedi, A. Basit, S. Besançon, C. Bommer, A. Esteghamati, K. Ogurtsova, P. Zhang, et al., Global and regional estimates and projections of diabetes-related health expenditure: Results from the international diabetes federation diabetes atlas, Diabetes research and clinical practice 162 (2020) 108072.

[3] D. S. Pisetsky, Pathogenesis of autoimmune disease, Nature Reviews Nephrology (2023) 1–16.

[4] L. Tang, S. J. Chang, C.-J. Chen, J.-T. Liu, Non-invasive blood glucose monitoring technology: a review, Sensors 20 (23) (2020) 6925.

[5] E. Shaffer-Hudkins, S. H. Orbeck, K. Bradley-Klug, N. Johnson, The diabetes simulation challenge: Enhancing patient perspective-taking for medical students, Diabetes Spectrum 35 (2) (2022) 150–158.

[6] T. K. Mathew, M. Zubair, P. Tadi, Blood glucose monitoring, StatPearls Publishing (2023 Jan).

[7] G. A. Silva, C. L. Souza, M. V. Oliveira, Teste oral de tolerância à glicose: solicitações desnecessárias e condições adequadas a realização do teste, Jornal Brasileiro de Patologia e Medicina Laboratorial 56 (2020).

[8] T. K. Mathew, P. Tadi, Blood glucose monitoring (2020).

[9] J. Pyl, E. Dendooven, I. Van Eekelen, M. den Brinker, H. Dotremont, A. France, K. Foubert, L. Pieters, J. Lambert, C. De Block, O. Aerts, Prevalence and Prevention of Contact Dermatitis Caused by FreeStyle Libre: A Monocentric Experience, Diabetes Care 43 (4) (2020) 918–920.

[10] T. Chang, H. Li, N. Zhang, X. Jiang, X. Yu, Q. Yang, Z. Jin, H. Meng, L. Chang, Highly integrated watch for noninvasive continual glucose monitoring, Microsystems & Nanoengineering 8 (1) (2022) 25.

[11] Q. Li, X. Xiao, T. Kikkawa, Noninvasive blood glucose level detection based on matrix pencil method and artificial neural network, Journal of Electrical Engineering & Technology 16 (2021) 2183–2190.

[12] J. Huang, Y. Zhang, J. Wu, Review of non-invasive continuous glucose monitoring based on impedance spectroscopy, Sensors and Actuators A: Physical 311 (2020) 112103.

[13] N. Ištuk, A. L. Gioia, H. Benchakroun, A. Lowery, B. McDermott, M. O'Halloran, Relationship between the conductivity of human blood and blood counts, IEEE Journal of Electromagnetics, RF and Microwaves in Medicine and Biology 6 (2) (2022) 184–190. doi:10.1109/JERM.2021.3130788.

[14] B. G. Pedro, D. W. C. Marcôndes, P. Bertemes-Filho, Analytical model for blood glucose detection using electrical impedance spectroscopy, Sensors 20 (23) (2020) 6928.

[15] B. G. Pedro, P. Bertemes-Filho, Glucose detection of ringer-lactate solution using

electrical bioimpedance: preliminary results, Journal of Physics: Conference Series 2008 (1) (2021) 012003. doi:10.1088/1742-6596/2008/1/012003.

[16] P. Bertemes Filho, Tissue characterisation using an impedance spectroscopy probe, Ph.D. thesis, University of Sheffield Thesis (2002).

[17] M. Darbas, J. Heleine, R. Mendoza, A. C. Velasco, Sensitivity analysis of the complete electrode model for electrical impedance tomography, Aims Mathematics 6 (7) (2021) 7333–7366.

[18] J. Rojas-Diaz, C. Felice, G. Ruiz, Continuous monitoring of conductivity using a uniform magnetic field, in: Journal of Physics: Conference Series, Vol. 1272, IOP Publishing, 2019, p. 012022.

[19] P. Bertemes-Filho, B. H. Brown, R. H. Smallwood, A. J. Wilson, Stand-off electrode (soe): a new method for improving the sensitivity distribution of a tetrapolar probe, Physiological Measurement 24 (2) (2003) 517.

[20] M. Mobarak, A review paper on the sensitivity analysis in bioimpedance measurement technique 7 (5) (2022) 346–350.

[21] V. X. Le, H. Lee, N. S. Pham, S. Bong, H. Oh, S.-H. Cho, I.-S. Shin, Stainless steel 304 needle electrode for precise glucose biosensor with high signal-to-noise ratio, Sensors and Actuators B: Chemical 346 (2021) 130552.

[22] U. Singh, P. K. Sharma, Study on geometric factor and sensitivity of subsurface for different electrical resistivity tomography arrays, Arabian Journal of Geosciences 15 (7) (2022) 560.

[23] J. A. Gómez-Sánchez, C. J. Felice, Description of corrections on electrode polarization impedance using isopotential interface factor, Journal of Electrical Bioimpedance 3 (1)

(2012) 29–35. doi:doi:10.5617/jeb.298.

[24] N. C. Hellige, B. Meyer, T. Rodt, J. Vogel-Claussen, G. Hahn, G. Hellige, In-vitro evaluation of contrast media for assessment of regional perfusion distribution by electrical impedance tomography (eit), Biomedical Engineering/Biomedizinische Technik 57 (SI-1-Track-B) (2012) 000010151520124442.

[25] K. Paduszyński, M. Okuniewski, U. Domańska, An effect of cation functionalization on thermophysical properties of ionic liquids and solubility of glucose in them–measurements and pc-saft calculations, The Journal of Chemical Thermodynamics 92 (2016) 81–90.

[26] J. Wei, Y. Tang, M. E. Ridgeway, M. A. Park, C. E. Costello, C. Lin, Accurate identification of isomeric glycans by trapped ion mobility spectrometry-electronic excitation dissociation tandem mass spectrometry, Analytical chemistry 92 (19) (2020) 13211–13220.

[27] G. El Mernissi, C. Barlet-Bas, C. Khadouri, S. Marsy, L. Cheval, A. Doucet, Characterization and localization of ouabain-insensitive na-dependent atpase activities along the rat nephron, Biochimica et Biophysica Acta (BBA)-Biomembranes 1064 (2) (1991) 205–211.

[28] S. Sikiru, N. Yahya, H. Soleimani, A. M. Ali, Y. Afeez, Impact of ionic-electromagnetic field interaction on maxwell-wagner polarization in porous medium, Journal of Molecular Liquids 318 (2020) 114039. doi:https://doi.org/10.1016/j.molliq.2020.114039.

[29] P. Høyum, H. Kalvøy, Ø. G. Martinsen, S. Grimnes, A finite element model of needle electrode spatial sensitivity, Physiological measurement 31 (10) (2010) 1369.

[30] O. I. Shuvo, M. N. Islam, Sensitivity analysis of the tetrapolar electrical impedance measurement systems using comsol multiphysics for the non-uniform and inhomogeneous

medium, Dhaka University Journal of Science 64 (1) (2016) 7–13.

Declaration of interests

The authors declare the following financial interests/personal relationships which may be considered as potential competing interests:

Bruna Gabriela Pedro reports financial support was provided by University of Santa Catarina State College of Technological Science. If there are other authors, they declare that they have no known competing financial interests or personal relationships that could have appeared to influence the work reported in this paper.

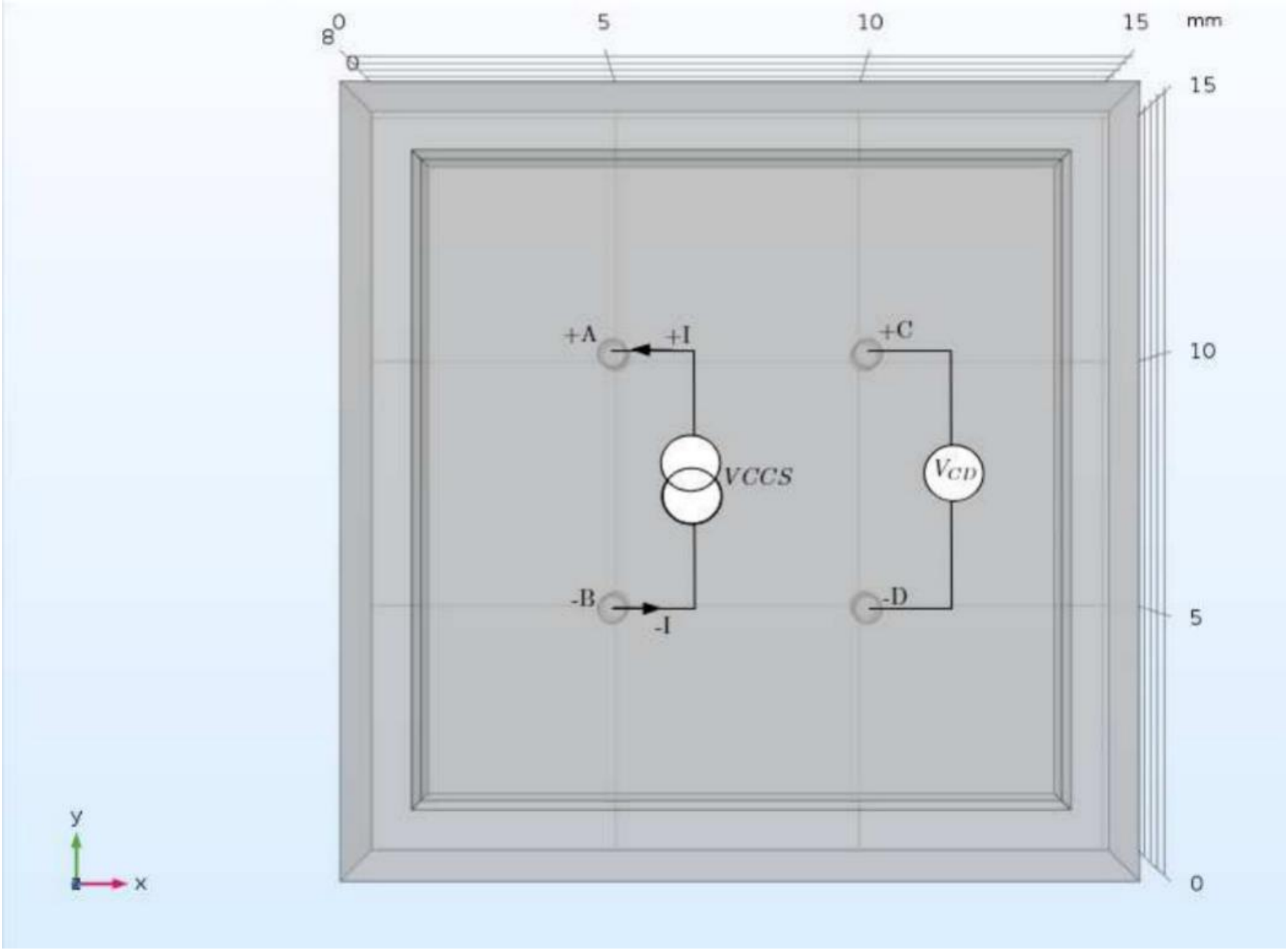

Figure 1

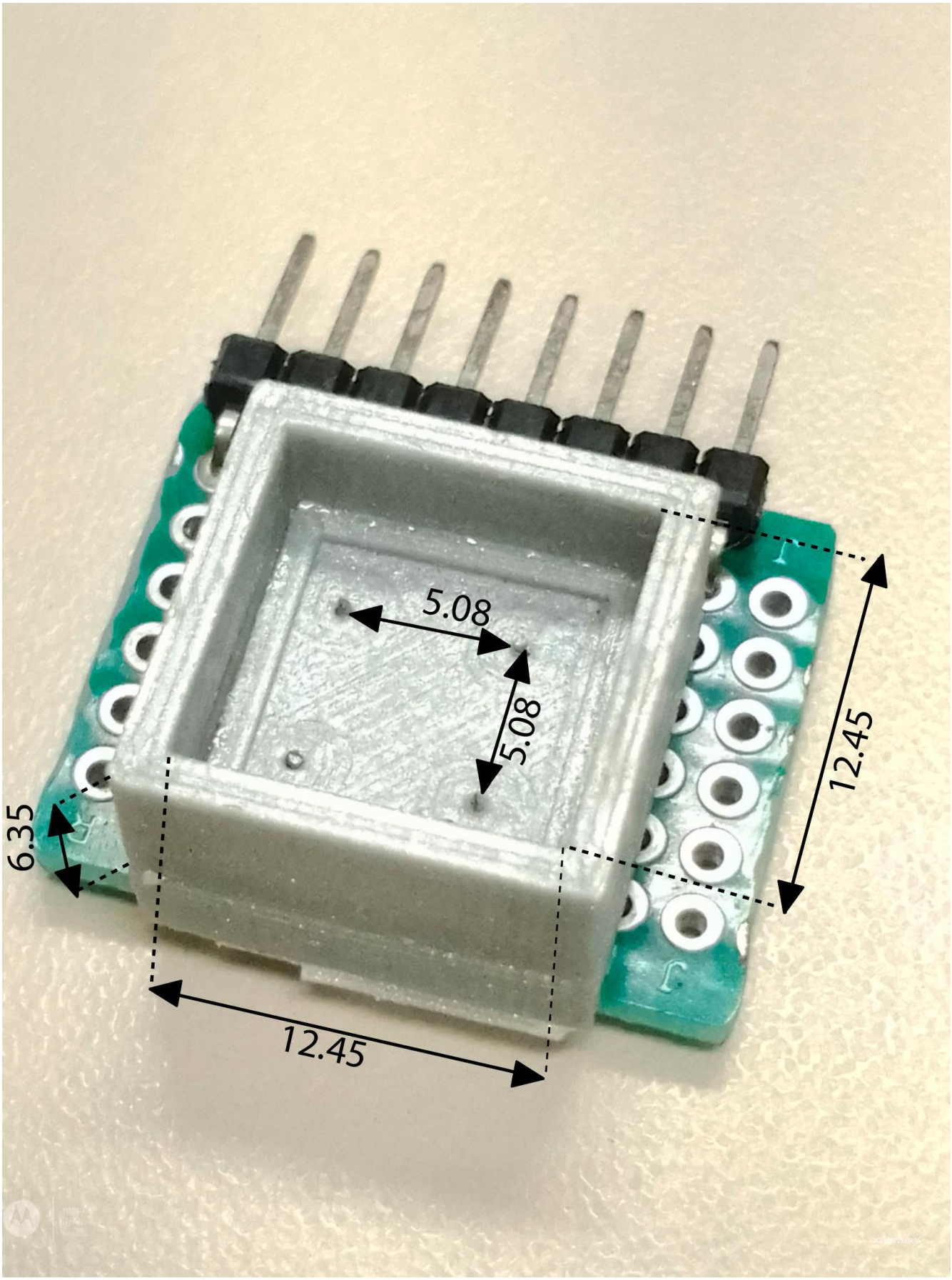

Figure 2

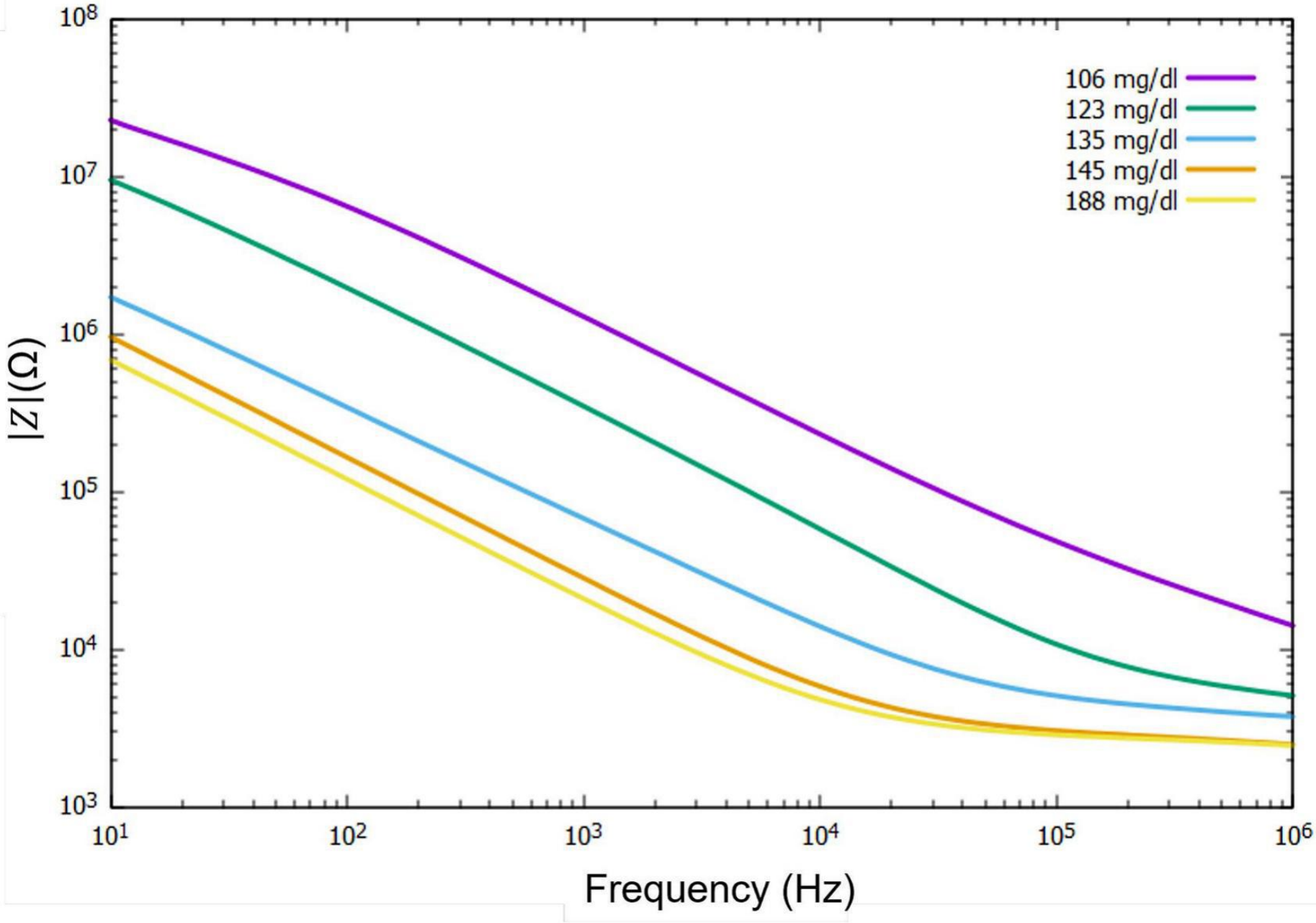
106 mg/dl
123 mg/dl
135 mg/dl
145 mg/dl
188 mg/dl
|Z|(Ω)
Frequency (Hz)
10^8
10^7
10^6
10^5
10^4
10^3
10^1
10^2
10^3
10^4
10^5
10^6

Figure 3

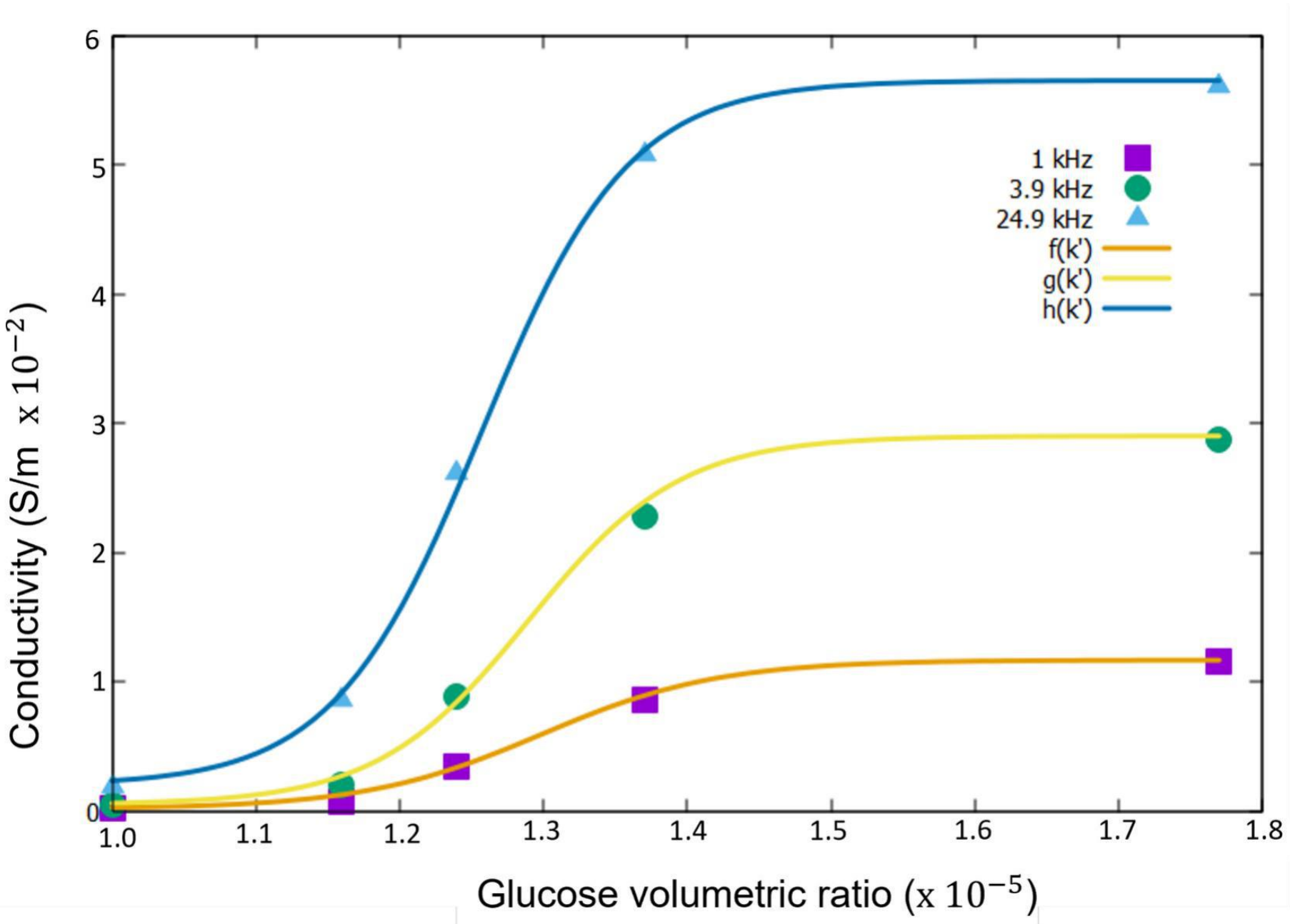
Conductivity (S/m x 10^{-2})
Glucose volumetric ratio (x 10^{-5})
1 kHz
3.9 kHz
24.9 kHz
f(k')
g(k')
h(k')
0
1
2
3
4
5
6
1.0
1.1
1.2
1.3
1.4
1.5
1.6
1.7
1.8

Figure 4

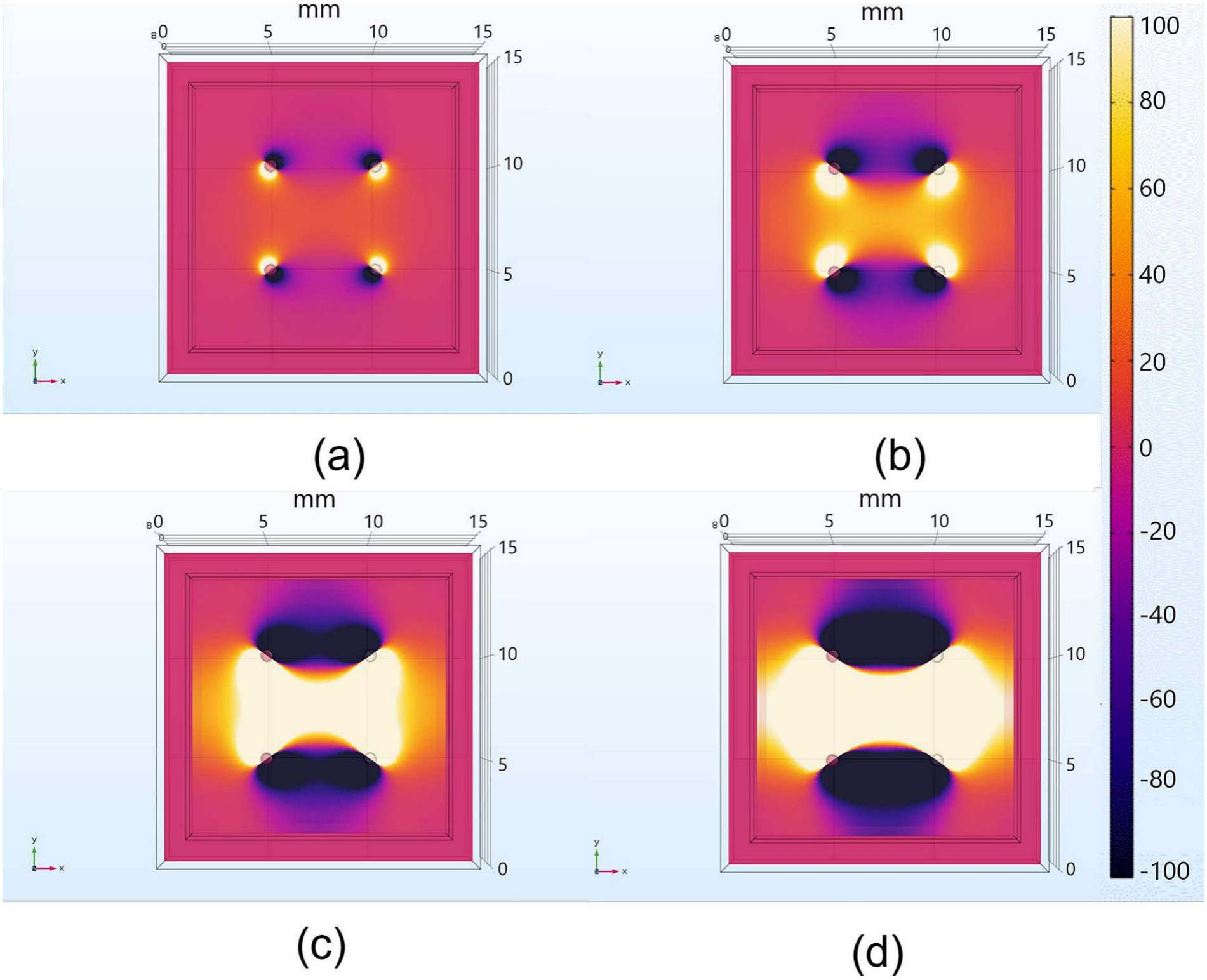

Figure 5

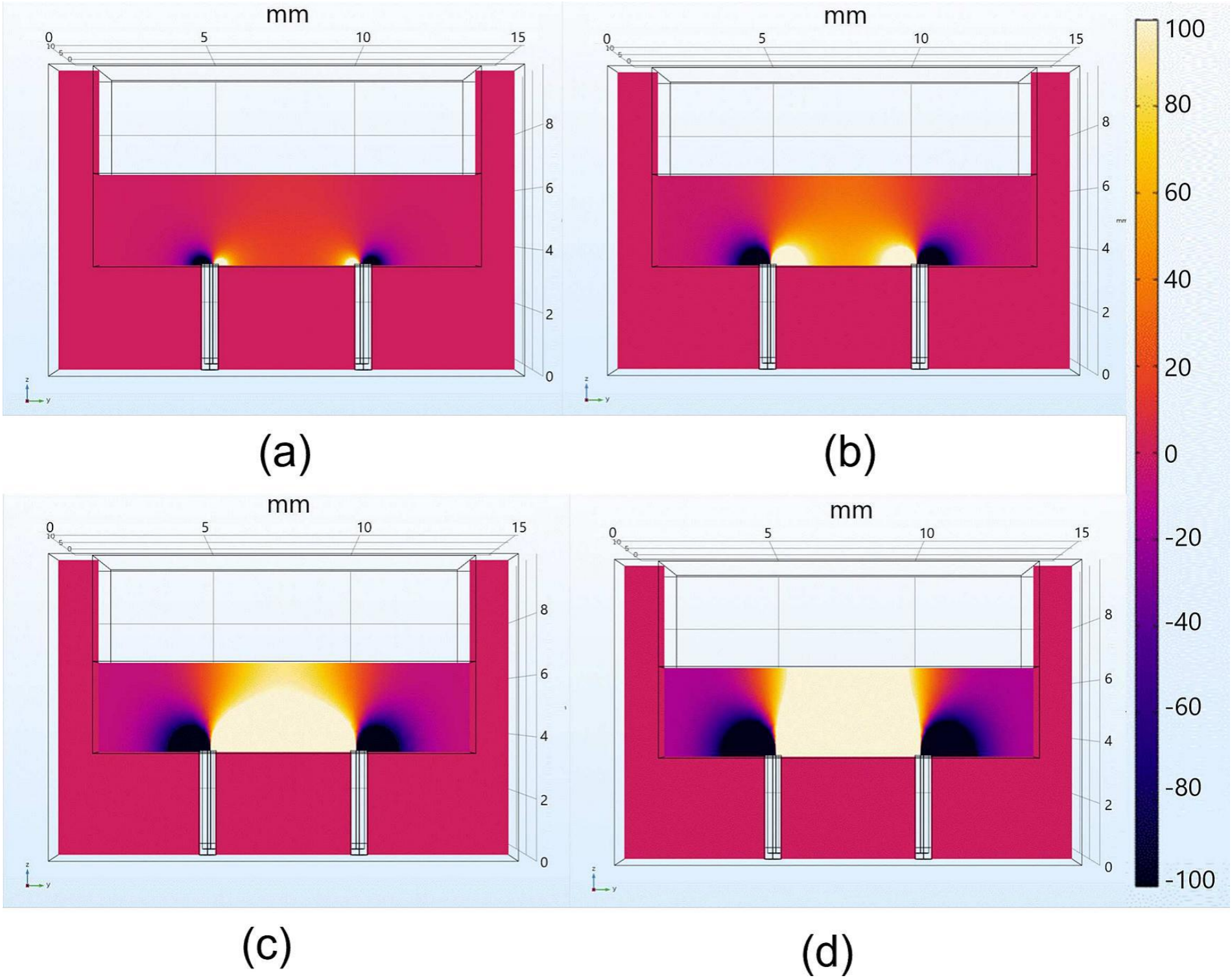

Figure 6

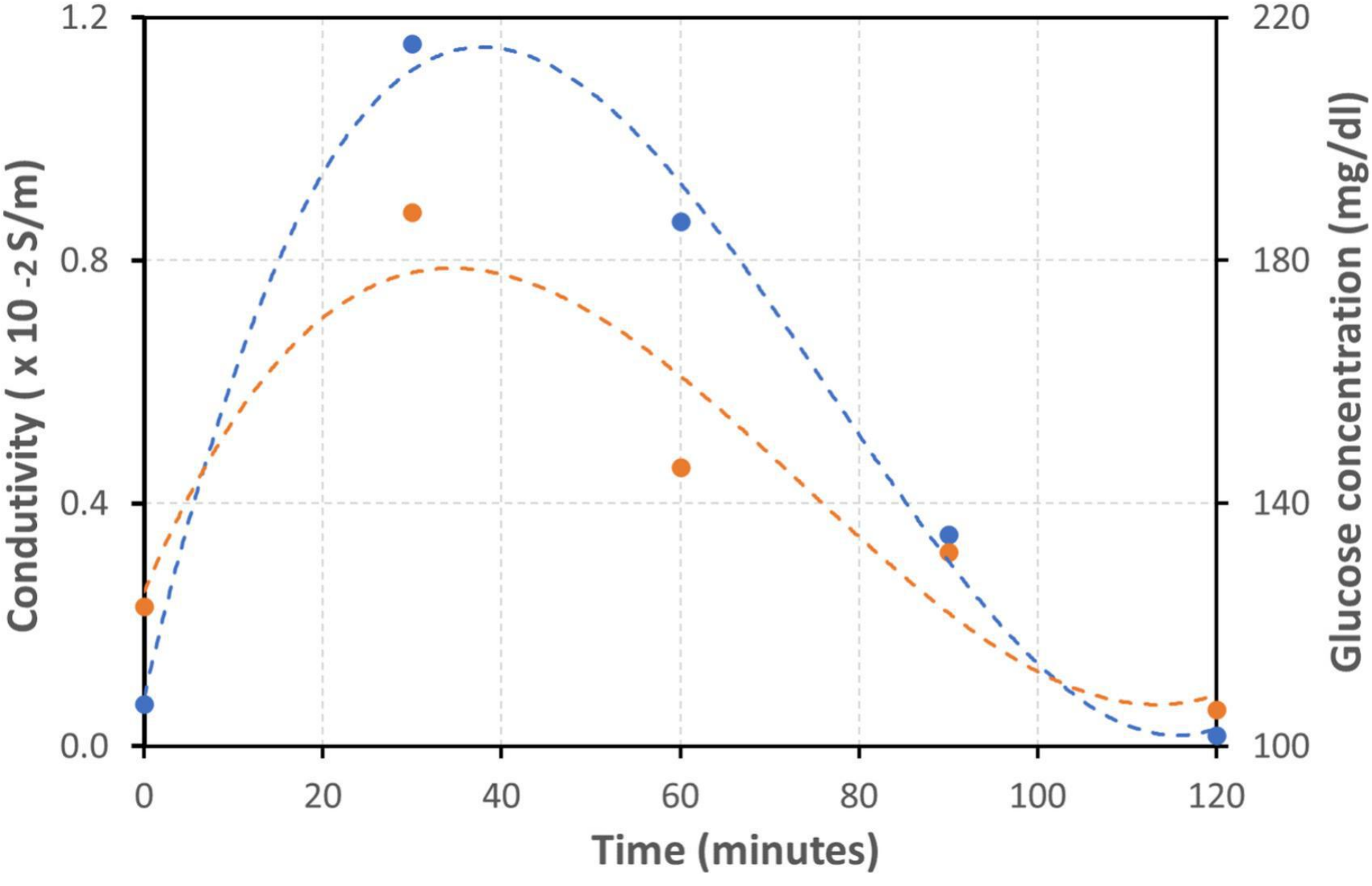
1.2
0.8
0.4
0.0
Condutivity (x 10 -2 S/m)
220
180
140
100
Glucose concentration (mg/dl)
0
20
40
60
80
100
120
Time (minutes)

Figure 7

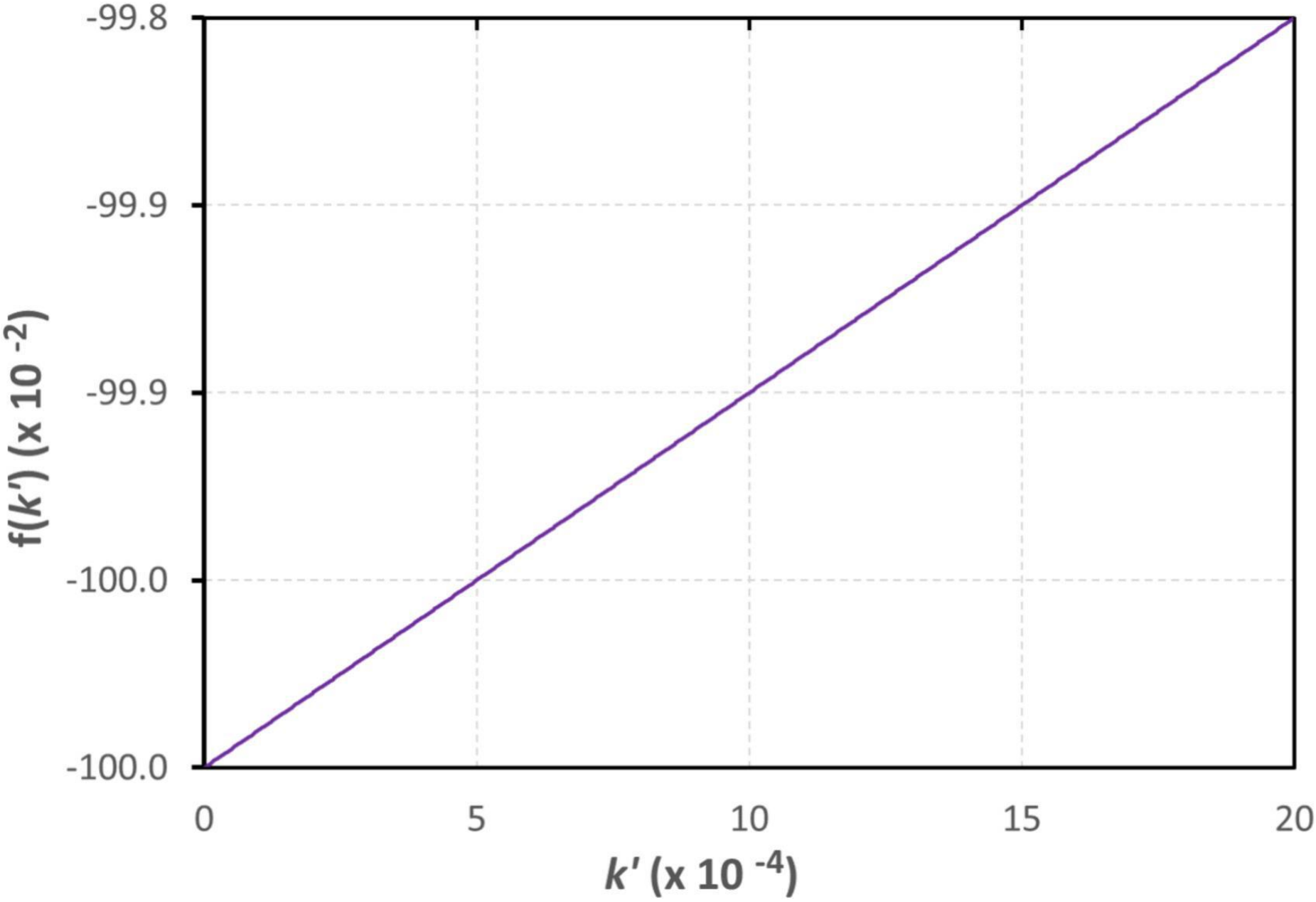

Figure 8

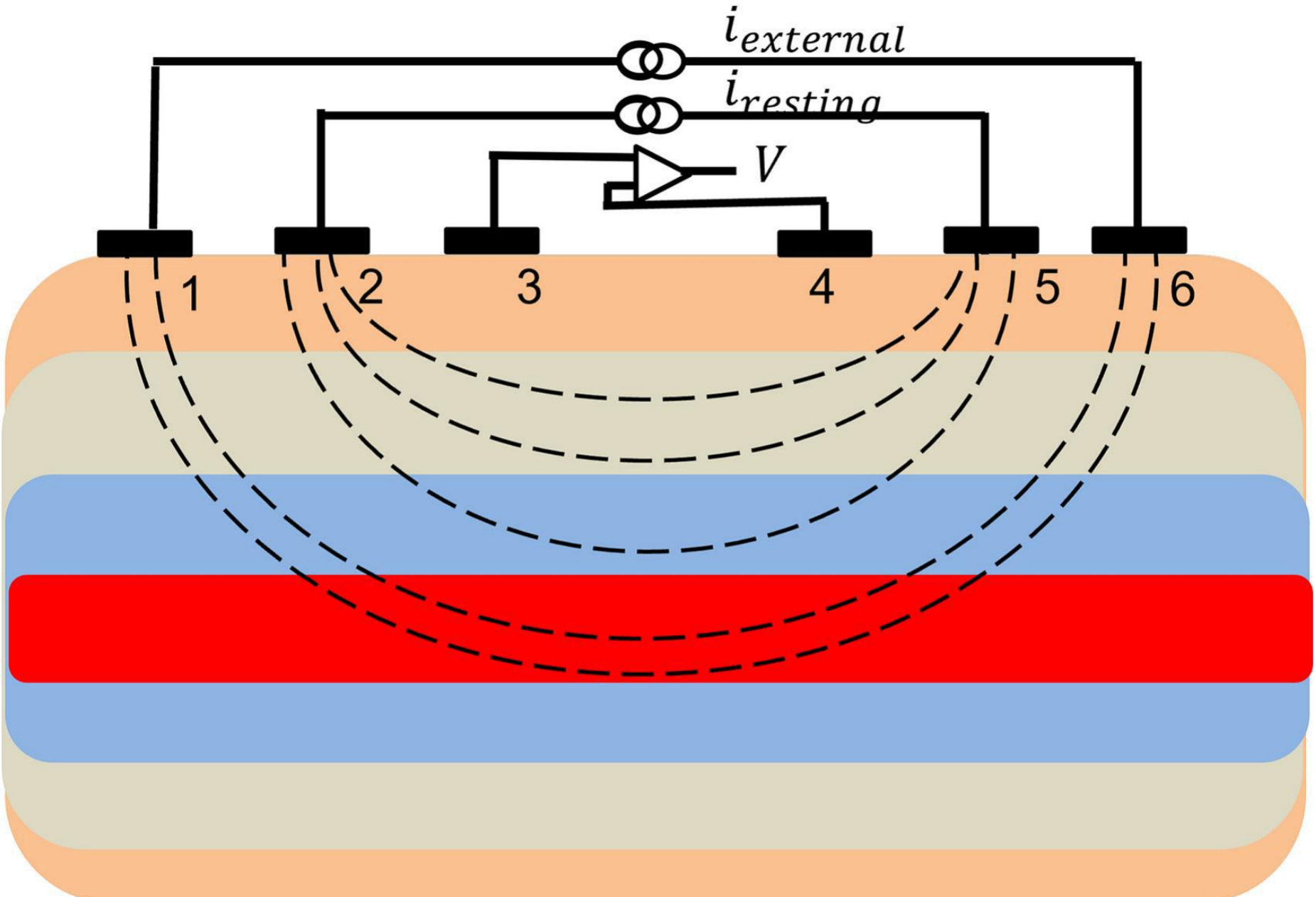

Figure 9